Photoejection of Electrons from Cycloocta[1,2,3,4-*def*;5,6,7,8-*d′e′f′*]bisbiphenylene Radical-Anion and Dianion Derivatives: Identification of a Light-Induced Disproportionation

Roy Shenhar,[†] Itamar Willner,*[,†] Andrzej Rajca,[‡] and Mordecai Rabinovitz[†]

Institute of Chemistry, The Hebrew University of Jerusalem, Jerusalem 91904, Israel, and Department of Chemistry, University of Nebraska, Lincoln, Nebraska 68588-0304

Received: November 27, 2001; In Final Form: April 24, 2002

Photoejection of electrons from 2,5,8,11-tetra-*tert*-butylcycloocta[1,2,3,4-*def*;5,6,7,8-*d′e′f′*]bisbiphenylene radical anion, $BPD^{\bullet-}$, and the respective dianion, BPD^{2-}, are described. Photoejection of an electron from BPD^{2-} yields a $[BPD^{\bullet-}\cdots e^-]$ cage complex and separated $BPD^{\bullet-}$ and e^-/Li^+ species. Recombination of the cage photoproducts proceeds at room temperature with a rate constant of $k^1_{rec} = (7.0 \pm 0.2) \times 10^5\ s^{-1}$, and the separated photoproducts recombine by a diffusional back-electron-transfer rate constant of $k^2_{rec} = (1.5 \pm 0.2) \times 10^9\ M^{-1}\cdot s^{-1}$. Photoejection of the electron from $BPD^{\bullet-}$ yields the neutral π-system, BPD, and the ejected electron reduces an unreacted $BPD^{\bullet-}$ to form BPD^{2-}. The photoejection of the electron from $BPD^{\bullet-}$ thus yields the disproportionation products, BPD and BPD^{2-}. The disproportionation products recombine by a diffusional process, $k_{rec} = (1.0 \pm 0.2) \times 10^{10}\ M^{-1}\cdot s^{-1}$ (at room temperature).

Introduction

Anions of conjugated π-systems exhibit intrinsic electron-donor properties due to the occupation of LUMO level(s) of the neutral conjugated systems. Accordingly, the light-induced ejection of electrons from polycyclic conjugated carbanions has been the subject of extensive research efforts in past decades.[1−10] While the photoejection of electrons from neutral conjugated π-systems yields oppositely charged products that recombine rapidly due to the electrostatic attractive interactions, the light-induced electron ejection from polycyclic conjugated polyanions yields negatively charged photoproducts that exhibit an electrostatic repulsive barrier for recombination. The retardation of the back electron transfer of the negatively charged species formed by electron ejection from oligo-anionic π-conjugated systems allows secondary chemical transformations of the reactive species. In fact, this property was successfully applied to develop photogalvanic cells based on aromatic polyanions.[11]

Photoejection of electrons from polycyclic aromatic anions has been the subject of studies in frozen 2-methyltetrahydrofuran matrixes that enabled us to observe the characteristic electron absorbance in the near-IR region,[12−14] and the EPR spectrum of the electron photoejected.[13] Softening of the glass matrix by heating the sample from 77 to 98 K, or by irradiation of the frozen solution with IR light, results in the recombination of the photoproducts. These studies have clearly indicated that the mobility of the electrons in the softened environment is substantially higher than that of the anionic species of the π-system.[14]

Detailed pulse radiolysis and flash photolysis experiments on electron ejection from cyclic π-conjugated anions were reported by Szwarc,[5,8] Fox,[6] Giling,[2,4] and others.[9,10,15,16] These studies have provided quantitative information on the kinetics of recombination of the photoproducts generated by the light-induced electron ejection from the π-conjugated polyanions. Also, these studies have revealed the solvation states of the species and the interactions that exist between the ejected electron and cations in the solution that act as counterions to the anionic species. From these studies it was concluded that the photoejected electron tends to associate to a cation in a solution that forms a cation−electron reactive pair (e^-/M^+). The formation of the cation−electron pair is enhanced at higher temperatures and with larger cations.[2]

For example, Giling and co-workers have shown[4] that photoejection of an electron from a radical anion results in the primary formation of a cation−electron reactive species that recombines with the neutral hydrocarbon, formed upon the electron photoejection, to yield the ground-state radical anion.

The photoejection of electrons from polycyclic π-conjugated systems that undergo multiple charging to defined oligoanionic species is far less explored.[8,10] The difficulties to generate pure, well-characterized, polyanionic species of controlled charging introduce complexity to the characterization of the charge ejection in these systems. The study of electron-photoejection processes in such systems is, however, interesting, as it enables us to probe the recombination dynamics as a function of charge accumulated on the conjugated π-system, and eventually to identify disproportionation paths between the polycyclic anions that originate from the electron photoejection process. Recently, we reported on the photochemical ejection of an electron from the corannulene dianion−Li^+ system.[17] Although corannulene undergoes sequential reduction to the radical anion, dianion, trianion radical, and tetraanion, we were able to generate a pure assembly only of the corannulene dianion and to characterize the electron photoejection from the system. We found that electron photoejection from corannulene dianion (Cor^{2-}) results in an intimate $[Cor^{\bullet-}\cdots e^-]$ pair. The association of the photoejected electron with the Li^+−cation competes with the recombination of $[Cor^{\bullet-}\cdots e^-]$ in the cage of photoproducts. Formation of the e^-/Li^+ pair separates the cage complex of the

* Corresponding author. Tel: 972-2-6585272. Fax: 972-2-6527715. E-mail: willnea@vms.huji.ac.il.
† The Hebrew University of Jerusalem.
‡ University of Nebraska.

10.1021/jp014330x CCC: $22.00
Published on Web 06/04/2002

photoproducts and results in the slow back electron transfer between $Cor^{\bullet-}$ and the e^-/Li^+ species.

Here we wish to report on the photoinduced electron ejection from the radical anion and dianion derived from 2,5,8,11-tetra-*tert*-butylcycloocta[1,2,3,4-*def*;5,6,7,8-*d′e′f′*]bisbiphenylene, BPD (**1**). We identify a new chemical feature that accompanies the

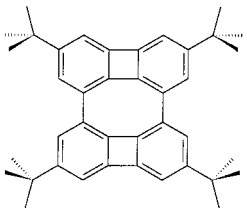

1

electron photoejection from the radical anion ($\mathbf{1}^{\bullet-}$), namely a photostimulated disproportionation of the photoproduct. In contrast to ground-state disproportionation that corresponds to a thermodynamic equilibrium process that is controlled by the redox potentials of the species, the photostimulated disproportionation process generated by electron ejection represents an unstable state that self-collapses by a back-electron-transfer reaction of the disproportionation products.

Experimental Section

Determination of Extinction Coefficient of BPD Anions. A glass apparatus was assembled to allow the accurate determination of the spectroscopic features of the respective anions under inert conditions. This apparatus consists of an ampule, a closed buret, and a 1-mm optical path quartz cell attached at the buret's top.

A weighted amount (within the accuracy of ± 0.002 mg) of ca. 2 mg of pure BPD was inserted into the ampule. The glass apparatus was then filled with argon; a lithium wire was freshly produced and directly inserted into the ampule, and immediately afterward the apparatus was connected to a vacuum line. The whole line and the glassware were flame-dried under vacuum. Previously distilled (and dried over a sodium−potassium alloy) tetrahydrofuran (THF) was vacuum-transferred to the buret part of the glassware. Degassing was performed by the freeze−pump−thaw method, and the apparatus was then flame-sealed under less than 0.01 mbar pressure.

When a small amount of THF was transferred to the ampule, the BPD dissolved completely, and the resulting solution was allowed to react with the lithium wire. After a short time interval the solution changed its color from orange to purple, which indicated the formation of the radical anion. The whole apparatus was then washed with the solution in order to dry the glass from trace amounts of moisture. This was usually observed by the disappearance of the purple color. Transferring the solution to the ampule and concentrating it (by vacuum transfer of most of the solvent to the buret part) allowed a further contact of the solution with the metal, which regenerated the radical anion.

After the purple color persisted in solution upon the repeated treatment of the BPD solution as described, the reduction of the sample was performed with a fixed volume of the solvent in order to maintain a constant concentration of the anionic species through the experiment. To determine the accurate point in time at which most of the BPD has been converted to its radical anion, the UV−vis spectrum of the solution was measured several times through the course of reduction. The recorded spectra showed the gradual decrease in the absorbance of BPD, with the concomitant enhancement of the absorbance bands characteristic to $BPD^{\bullet-}$. Plotting the OD at λ_{max} of the radical anion against time yielded a curve exhibiting a maximum OD value at a certain time. The UV−vis spectrum recorded at this time interval shows only the absorbance bands[18] of the radical anion $BPD^{\bullet-}$ (with no susperimposed band characteristic to the neutral substrate BPD). Accordingly, it is assumed that under these conditions all BPD is transformed to $BPD^{\bullet-}$.

The same method was applied for the determination of the absorbance features of the BPD dianion, BPD^{2-} (yellow-brown solution), assuming that the maximum of the OD vs time (acquired at λ_{max} of BPD^{2-}) is indeed indicative of a complete transformation from one reduction state to the next. This assumption is supported by NMR and UV−vis experiments, which reveal that when the dianion is visible, there is no neutral compound and no radical anion (which for even minute amounts of the latter would have extinguished the NMR peaks of the dianion).

Kinetics Measurements

Glassware. The glassware that was fabricated for the kinetics measurements consisted of two ampules and a 1-cm optical-path quartz fluorescence cell, arranged in parallel and connected to a central glass pipe that was attached at the cell's top. One ampule contained the lithium wire (the "reduction ampule"), and the other one was used for solvent vaccuum transfer (as the optical cell by itself is not suitable for vacuum distillation). This setup enabled performing the reduction at the high concentrations required and, on the other hand, to dilute the resulting anionic solution in the optical cell to comply with the low optical density required for the flash-photolysis experiment. The dilution of the sample was performed by transferring a small portion of the material to the optical cell while retaining the rest in the second ampule, distilling the solvent to the "reduction ampule" (by cooling it with liquid nitrogen) and afterward transferring it to the optical cell by tilting the glass apparatus.

UV−Vis Flash Photolysis System. A Nd:YAG laser (Continuum Surelite I), equipped with second and third harmonic crystals was used as the base light source. The 355-nm third harmonic light source (1 Hz repetition rate, ∼150 mJ/pulse, 5.5 ns pulse width) was used to pump an optical parametric oscillator (Continuum Surelite OPO), resulting in monochromatic light pulses within the visible range (300−700 nm) at a constant power output of 20−25 mJ/pulse (wavelength dependent). The excitation of the BPD anions was performed at their characteristic absorbance maxima ($\lambda_{max} = 452$ or 593 nm for the radical anion, and $\lambda_{max} = 462$ nm for the dianion), to obtain the optimal results. The excitation pulses hit the sample chamber while the analytical light source analyzes the spectral changes in the sample chamber in a perpendicular configuration.

The analytical light source for probing the absorbance changes in the sample as a result of the laser pulse excitation was a pulsed Xe arc lamp. Since the absorbance transients of some of the species were in the millisecond time scale, pulsing the analytical lamp was applied only for probing the fast transient components. Noise reduction for the entire curve (i.e., over the entire time-range) was achieved by electronic amplification of the acquired signal with a 1 kΩ resistor and using a narrow bandwidth on the digitizing oscilloscope.

The spectral changes were recorded at room temperature by two complementary detection systems, which were interchangeable by changing the position of a mirror. One detection system consisted of a monochromator−photomultiplier (PMT) detection system combined with an oscilloscope (Infinium, model HP54810A). This detection system was used to follow transient

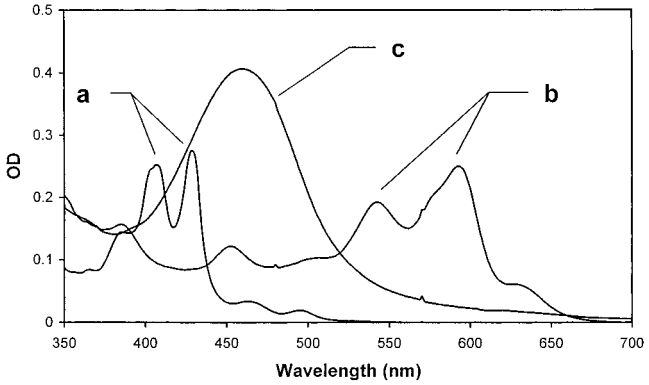

Figure 1. Steady-state absorption spectra of the species derived from BPD at different reduction states: (a) neutral state, BPD; (b) radical anion, $BPD^{\bullet -}$; (c) dianion, BPD^{2-}.

absorbances at a fixed wavelength. The data recorded with the oscilloscope were transferred to a RISC station for further processing and kinetic analysis (including nonlinear fits). The second detection system was an intensified charge coupling device detection system (ICCD), used to acquire a transient spectrum at a certain point in time after the laser pulse. The light passing through the sample was guided through an optical fiber, projected on a 150-grooves/mm grating (Acton Spectrometer, model SP-150) and reflected on the ICCD detector. The ICCD detector (Princeton Instruments) was cooled to −30 °C in order to increase its sensitivity. A controller (Princeton Instruments, model ST-130) controlled the ICCD's temperature and the data transfer to a personal computer, and a high voltage pulse generator (Princeton Instruments, model PG-200) was used to allow for exposure duration as short as 100 ns. An LKS.60 Spectrometer Control Unit (Applied Photophysics) served as the internal clock of the PMT detection system, and also controlled the synchronization of the other parts of the detection system. When the ICCD detection system was used, the laser functioned as the base timing source, and the synchronization of the ICCD detector with the laser was achieved with another LKS system (Applied Photophysics) coupled to a delay generator (Stanford).

Results and Discussion

2,5,8,11-Tetra-*tert*-butylcycloocta[1,2,3,4-*def*;5,6,7,8-*d′e′f′*]-bisbiphenylene (**1**), a biphenylene dimer, termed BPD, has been reduced in the past to the respective radical anion and dianion using lithium or potassium as reducing metals.[18] Recently, we accomplished the sequential reduction of BPD to $BPD^{\bullet -}$, BPD^{2-}, and $BPD.^{4-}$ We have demonstrated that BPD^{4-} forms supramolecular clusters of helical structures.[19] The polycyclic conjugated compound **1** includes a cyclobutadiene-type ring and a cyclooctatetraene ring and yet exists in an almost planar structure. NMR investigations and quantum mechanical calculations indicate that BPD exhibits enhanced aromaticity upon transformation from the neutral to the dianion, BPD^{2-},[20] as is generally expected from a $(4n+2)\pi$-electron dianion.

Figure 1 shows the absorbance spectrum of the neutral BPD (**1**), curve a, and the absorbance spectra of the radical anion, $BPD^{\bullet -}$, and the dianion, BPD^{2-}, formed upon the stepwise reduction of **1** with Li, curves b and c, respectively. We calculate the following extinction coefficients for BPD (**1**): λ(429 nm), $\epsilon = 9200\ M^{-1}\cdot cm^{-1}$; λ(409 nm), $\epsilon = 7000\ M^{-1}\cdot cm^{-1}$. Figure 2a,b shows the time-dependent absorbance changes at $\lambda = 593$ nm and $\lambda = 462$ nm for $BPD^{\bullet -}$ and BPD^{2-}, respectively. From

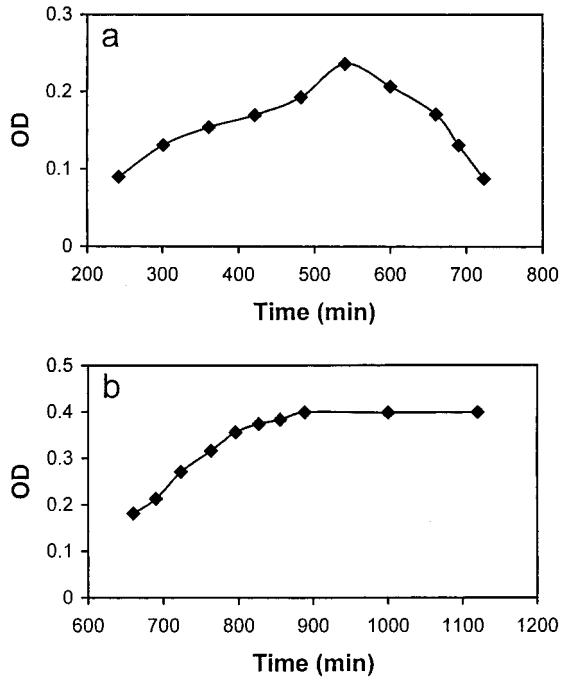

Figure 2. Time-dependent absorbance changes of (a) $BPD^{\bullet -}$ (at $\lambda =$ 593 nm) and (b) BPD^{2-} (at $\lambda = 462$ nm), upon reduction with lithium.

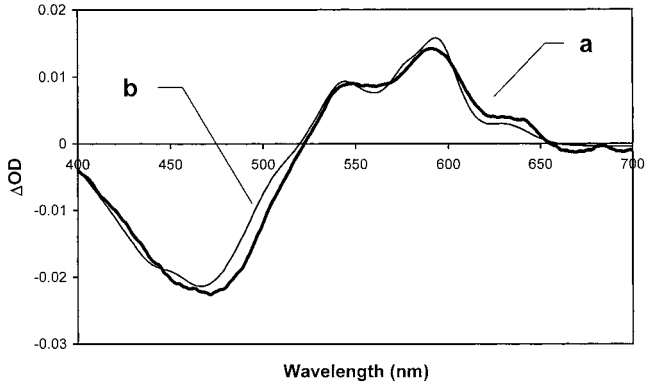

Figure 3. (a) Transient absorbance spectrum of the irradiated BPD^{2-} solution (excitation at $\lambda = 462$ nm). The spectrum is acquired 70 ns after the laser pulse. The bleaching of the dianion is observed at $\lambda =$ 462 nm, and the transient formation of the radical anion is reflected as positive ΔOD at 593, 542, and 630 nm. (b) Simulated absorbance spectrum obtained upon subtraction of the steady-state absorption spectrum of BPD^{2-} from that of $BPD^{\bullet -}$ (normalized to the yield of the photoprocess).

the absorbance spectra of $BPD^{\bullet -}$ and BPD^{2-}, which correspond to the maxima in Figure 2a,b, we calculate the following extinction coefficients for $BPD^{\bullet -}$ and BPD^{2-}. For $BPD^{\bullet -}$, λ(593 nm), $\epsilon = 7000\ M^{-1}\cdot cm^{-1}$ and λ(542 nm), $\epsilon = 5300\ M^{-1}\cdot cm^{-1}$. For BPD^{2-}, λ(462 nm), $\epsilon = 11\,300\ M^{-1}\cdot cm^{-1}$.

Photoexcitation of the BPD^{2-} solution (approximate concentration 4×10^{-5} M) yields the transient absorption spectrum shown in Figure 3, curve a. A bleached absorbance band at 462 nm is detected, and the formation of two absorbance bands at 542 nm (lower intensity) and 593 nm (higher intensity) together with a shoulder at ca. 630 nm are observed. The bleached absorption bands clearly indicate the transient disappearance of the dianion, BPD^{2-}, whereas the generated transient absorption bands imply that the radical anion $BPD^{\bullet -}$ is formed. These results clearly indicate that photoejection of an electron from BPD^{2-} occurred, resulting in $BPD^{\bullet -}$. Figure 3, curve b, shows a calculated spectrum that corresponds to the

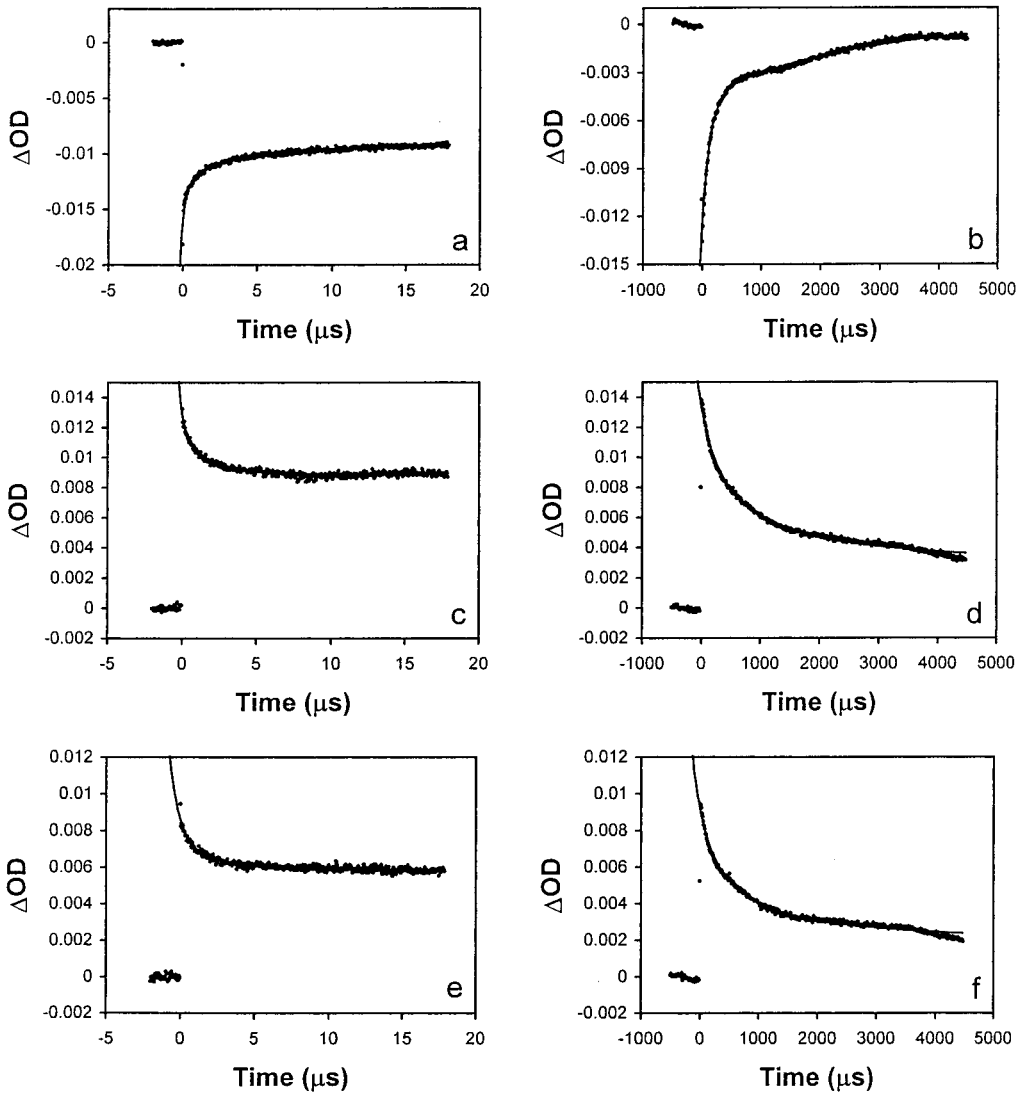

Figure 4. Transient Absorbance curves detected at different time scales and corresponding to the photoejection of the electron from BPD^{2-}: (a) and (b) recovery of the BPD^{2-}, monitored at 462 nm; (c) and (d) depletion of $BPD^{\bullet-}$, monitored at $\lambda = 593$ nm; (e) and (f) depletion of $BPD^{\bullet-}$, monitored at 542 nm.

subtraction of the spectrum of BPD^{2-} from that of $BPD^{\bullet-}$ (cf. Figure 1, curves c and b, respectively) using a normalization factor of 0.07 that corresponds to the yield of the photoinduced electron ejection. We observe an excellent overlap of the simulated spectrum and the experimental transient. This result supports the conclusion that photoexcitation of BPD^{2-} results in the photoejection of an electron, and the formation of $BPD^{\bullet-}$.

Figure 4 shows the absorbance transients corresponding to the recovery of the bleached dianion recorded at $\lambda = 462$ nm (curves a and b), and to the depletion of the $BPD^{\bullet-}$ recorded at $\lambda = 593$ nm (curves c and d) and $\lambda = 542$ nm (curves e and f). The bleached BPD^{2-} is recovered by two independent processes that reveal significantly different kinetic features. A rapid recovery of the bleached BPD^{2-} is observed that proceeds for ca. 1.5 μs, Figure 4, curve a, followed by a substantially slower recovery of BPD^{2-} that proceeds on a time scale that is longer than 5 ms, Figure 4, curve b. Similarly, the depletion of the $BPD^{\bullet-}$ reveals two paths of different kinetics: A fast disappearance of $BPD^{\bullet-}$ occurring within ca. 1.5 μs, Figure 4, curves c and e, followed by a very slow decay of $BPD^{\bullet-}$ that occurs on a time scale of several milliseconds, Figure 4, curves d and f. In fact, similar kinetic features were observed upon analyzing the photoinduced electron ejection from corannulene dianion.[17] The rapid and slow depletion of $BPD^{\bullet-}$ (or recovery of BPD^{2-}) are attributed to the set of chemical transformations outlined in eqs 1−5. Photoexcitation of BPD^{2-} results in the

$$BPD^{2-} \xrightarrow{h\nu} [BPD^{2-}]^* \rightarrow [BPD^{\bullet-}\cdots e^-] \quad (1)$$

$$[BPD^{\bullet-}\cdots e^-] \xrightarrow{k^1_{rec}} BPD^{2-} \quad (2)$$

$$[BPD^{\bullet-}\cdots e^-] \xrightarrow{k_s} BPD^{\bullet-} + e^- \quad (3)$$

$$e^- + Li^+ \rightarrow e^-/Li^+ \quad (4)$$

$$BPD^{\bullet-} + e^-/Li^+ \xrightarrow{k^2_{rec}} BPD^{2-} + Li^+ \quad (5)$$

photoejection of an electron, and the formation of the cage of photoproducts $[BPD^{\bullet-}\cdots e^-]$, eq 1. Back electron transfer of the intimate pair of photoproducts in the cage structure leads to the rapid disappearance of $BPD^{\bullet-}$ (or fast recovery of BPD^{2-}), eq 2. The separation of the primary cage structure of the photoproducts, eq 3, is followed by the rapid formation of an e^-/Li^+ pair ($>10^{12}$ $M^{-1}\cdot s^{-1}$),[3−5] eq 4, which acts as the active species for the diffusional recombination of the electron with

$BPD^{\bullet-}$. Analysis of the slow and fast transients yields the recombination rate-constants: $k^1_{rec} = (7.0 \pm 0.2) \times 10^5\ s^{-1}$ and $k^2_{rec} = (1.5 \pm 0.2) \times 10^9\ M^{-1}\cdot s^{-1}$. The rate constant for the separation of the primary cage complex of photoproducts is calculated to be $k_s = 1.6 \times 10^6\ s^{-1}$.

Photoejection of an electron from the radical anion, $BPD^{\bullet-}$, has been similarly studied. Figure 5, curve a, shows the transient absorption spectrum obtained upon the photoexcitation of $BPD^{\bullet-}$. The absorption bands at ca. 540 and 590 nm and the shoulder at 630 nm are bleached, implying that photoexcitation of $BPD^{\bullet-}$ results in the depletion of the radical anion. In analogy to the photoexcitation of other polycyclic conjugated anions, we may assume that photoexcitation of $BPD^{\bullet-}$ leads to electron ejection and to the formation of the neutral BPD. Accordingly, we attempted to simulate the transient absorption spectrum by assuming the photoejection of the electron as the sole process in the system. Figure 5, curve b shows the calculated transient spectrum that corresponds to the subtraction of the spectrum of $BPD^{\bullet-}$ from the spectrum of the neutral species, BPD. This spectral subtraction basically corresponds to the electron photoejection process (the subtraction process uses a normalization factor of 0.10 that corresponds to the electron photoejection yield). The calculated transient spectrum, Figure 5, curve b, does not overlap the experimental spectrum, indicating that photoejection of the electron does not simply yield the neutral product, BPD. If only the neutral product BPD is formed, one would expect to observe two absorbance bands at 429 and 409 nm, with an optical density comparable to the bleached bands of $BPD^{\bullet-}$. (cf. Figures 1 and 5, curve b). Close inspection of the experimental transient obtained upon the photoejection of the electron from $BPD^{\bullet-}$ reveals a positive absorbance band at ca. 460 nm that might be ascribed to the dianion BPD^{2-} (cf. Figure 1, curve c). Thus, we explain the results by the set of transformations outlined in eqs 6−9. Photoexcitation of $BPD^{\bullet-}$

$$BPD^{\bullet-} \xrightarrow{h\nu} [BPD^{\bullet-}]^* \rightarrow [BPD\cdots e^-] \quad (6)$$

$$[BPD\cdots e^-] \rightarrow BPD + e^- \quad (7)$$

$$e^- + Li^+ \rightarrow e^-/Li^+ \quad (8)$$

$$BPD^{\bullet-} + e^-/Li \rightarrow BPD^{2-} + Li^+ \quad (9)$$

leads to electron ejection and the formation of the cage complex of the neutral BPD and the ejected electron, eq 6. Separation of the complex followed by complexation of the electron with Li^+ yields the reactive electron in the system, eqs 7 and 8. Since the photoejection of the electron proceeds with a yield of only ca. 10%, the separated electron is in an environment rich with nonreacted $BPD^{\bullet-}$. Reduction of $BPD^{\bullet-}$ by the electron would then yield the dianion BPD^{2-}, eq 9, consistent with the observed absorbance band in the transient spectrum at $\lambda = 460$ nm. This analysis leads to an important conclusion that photoexcitation of $BPD^{\bullet-}$ and the electron ejection leads to the neutral and dianionic products, BPD and BPD^{2-}. That is, photoejection of the electron from $BPD^{\bullet-}$ leads to the disproportionation products BPD and BPD^{2-}. Furthermore, the analysis of the transient absorbance spectrum suggests that one $BPD^{\bullet-}$ unit is transformed to BPD whereas the second $BPD^{\bullet-}$ unit is depleted by its reduction with the separated electron to BPD^{2-}. This explanation provides a nice support to the fact that the positive absorbance bands at ca. 430 and 460 nm corresponding to BPD and BPD^{2-}, respectively, exhibit an optical density that is ca. half that of the bleached $BPD^{\bullet-}$. Figure 5, curve c, shows the

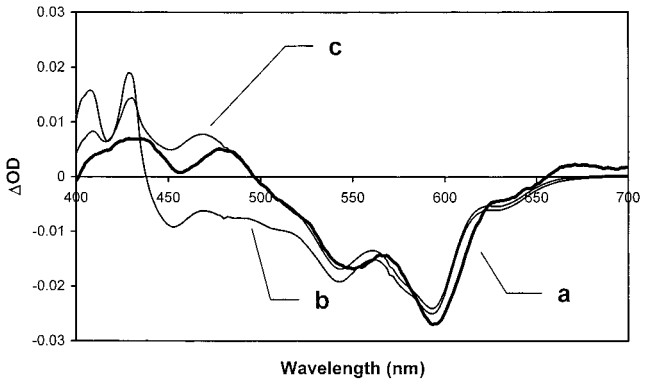

Figure 5. (a) Transient absorption spectrum of the irradiated $BPD^{\bullet-}$ solution (excitation at $\lambda = 452$ nm), acquired 70 ns after the laser pulse. The bleaching of the radical anion can be observed at $\lambda = 542$, 593, and 630 nm, and the transient formation of the neutral BPD and BPD^{2-} are reflected as positive ΔOD at ca. 430 and 460 nm, respectively. (b) Simulated spectrum assuming electron photoejection from $BPD^{\bullet-}$ as the sole process in the system, obtained upon subtraction of the steady-state absorption spectrum of $BPD^{\bullet-}$ from that of neutral BPD (normalized to the yield of the photoprocess). (c) Simulated absorption spectrum corresponding to the subtraction of the steady-state absorption spectrum of $BPD^{\bullet-}$ (2-fold concentration) from the sum of the spectra of neutral BPD and BPD^{2-} (normalized to the yield of the photoprocess).

simulated transient absorption spectrum that corresponds to the subtraction of the spectrum of $BPD^{\bullet-}$ (2-fold concentration) from the sum of the spectra of BPD and BPD^{2-}, $2\cdot OD(BPD^{\bullet-}) - [OD(BPD) + OD(BPD^{2-})]$. The simulated spectrum overlaps nicely the experimental transient supporting the analysis that photoexcitation of $BPD^{\bullet-}$ yields as photoproducts the disproportionation components BPD and BPD^{2-}, respectively.

Figure 6 shows the transient absorbance curves corresponding to the recombination of the photoproducts formed after the photoejection of the electron from $BPD^{\bullet-}$. Figure 6, curves a and b, show the recovery of the bleached radical anion followed at 542 and 593 nm, respectively. Figure 6, curves c and d, show the disappearance of the photogenerated neutral species, BPD, monitored at two wavelengths, $\lambda = 409$ nm and $\lambda = 429$ nm, respectively. Figure 6, curve e, shows the transient that corresponds to the depletion of the transiently generated BPD^{2-} at $\lambda = 462$ nm. The inspection of the set of transients and their kinetic analysis reveal several important features: (i) Kinetic analysis of the different transients indicates that all of the processes follow a bimolecular kinetics. (ii) Bimolecular rate constant values that are calculated from curve (a) and (b) of Figure 6 (acquired at the characteristic wavelengths of $BPD^{\bullet-}$) are approximately half those calculated for BPD and BPD^{2-} from the other curves. This implies that the disappearance of BPD and BPD^{2-} and the recovery of $BPD^{\bullet-}$ are inter-related processes via a recombination of the disproportionation products, that generates 2 equiv of $BPD^{\bullet-}$, eq 10. The rate constant

$$BPD + BPD^{2-} \xrightarrow{k_{rec}} 2BPD^{\bullet-} \quad (10)$$

calculated for this process is $k_{rec} = (1.0 \pm 0.2) \times 10^{10}\ M^{-1}\cdot s^{-1}$. (iii) The recombination rate constant of the photoproducts, k_{rec}, is ca. 7-fold higher than the back-electron-transfer rate constant observed between the separated electron (e^-/Li^+) and the $BPD^{\bullet-}$ or corannulene radical anion[17] formed upon the photoejection of the electron from BPD^{2-} or corannulene dianion (Cor^{2-}), respectively. This observation may be attributed to the fact that recombination between BPD and BPD^{2-}, eq 10, occurs between a neutral and a dianionic species. In the latter system, no repulsive interactions between the photoproducts exist. On the

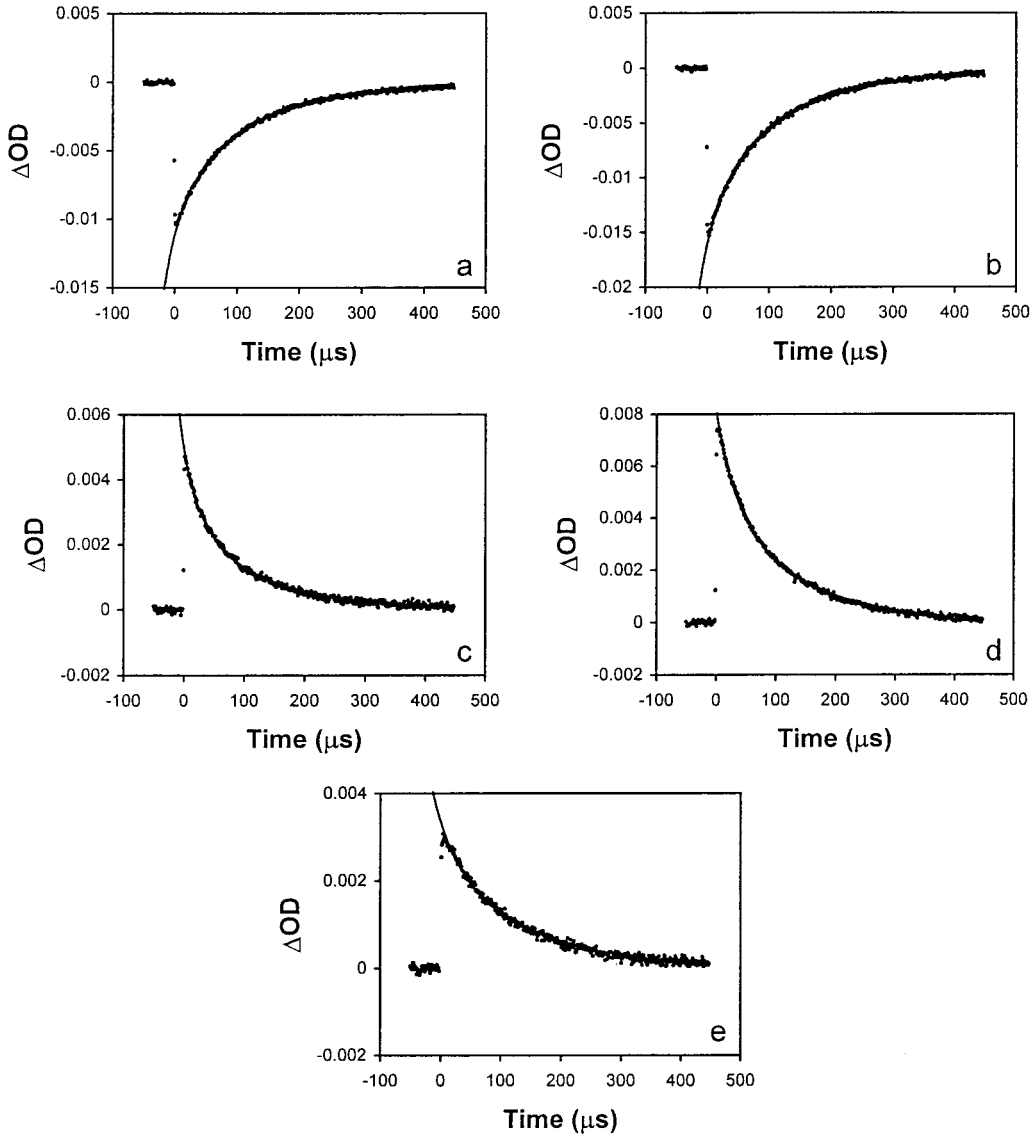

Figure 6. Transient absorbance curves corresponding to the light-induced disproportionation of $BPD^{\bullet-}$ upon electron ejection: (a) and (b) recovery of the $BPD^{\bullet-}$, monitored at 542 and 593 nm, respectively; (c) and (d) decay of BPD, monitored at 409 and 429 nm, respectively; (e) depletion of BPD^{2-}, monitored at $\lambda = 462$ nm.

other hand, recombination of the e^-/Li^+ with $BPD^{\bullet-}$ or $Cor^{\bullet-}$ is accompanied by electrostatic repulsive interactions leading to the slower recombination rates.

Conclusions

The present study has elucidated the photochemical electron ejection processes from BPD^{2-} and $BPD^{\bullet-}$. The electron photoejection from the dianion BPD^{2-} follows the usual path observed for other anionic π-conjugated polycyclic compounds, i.e., formation of an intimate cage complex with the ejected electron, separation of the primary cage complex, and diffusional recombination of the photoproducts. Analysis of the electron photoejection process from $BPD^{\bullet-}$ revealed, however, a new mechanistic path where the electron ejection process yields the disproportionation of $BPD^{\bullet-}$ to BPD^{2-} and neutral BPD. This light-stimulated disproportionation of $BPD^{\bullet-}$ should be considered as a model concept for studying photoinduced disproportionation reactions in other radical anion systems. Previous studies have demonstrated the photoinduced disproportionation of an electron-transfer photoproduct by means of a two-phase system.[21] This latter disproportionation system represents, however, a thermodynamically equilibrated assembly. The light-induced generation of the disproportionation products of $BPD^{\bullet-}$, by the electron photoejection process, represents, however, an endoergic route. The energy stored in the disproportionation products is released by recombination to $BPD^{\bullet-}$.

Acknowledgment. This research was supported by THE Israel SCIENCE FOUNDATION (grant no. 147/002), and by the Enrique Berman Foundation, The Hebrew University of Jerusalem. R.S. thanks Julian Wasserman for technical assistance.

References and Notes

(1) Eloranta, J.; Linschitz, H. *J. Chem. Phys.* **1963**, *38*, 2214.
(2) Giling, L. J.; Kloosterboer, J. G.; Rettschnick, R. P. H.; van Voorst, J. D. W. *Chem. Phys. Lett.* **1971**, *8*, 457.
(3) Rämme, G.; Fisher, M.; Claesson, M.; Szwarc, M. *Proc. R. Soc. London A* **1972**, *327*, 467.
(4) Giling, L. J.; Kloosterboer, J. G. *Chem. Phys Lett.* **1973**, *21*, 127.
(5) Szwarc, M.; Levin, G. *J. Photochem.* **1976**, *5*, 119.
(6) Fox, M. A. *Chem. Rev.* **1979**, *79*, 253 and references therein.
(7) Soumillion, J. P. *Top. Curr. Chem.* **1993**, *168*, 93 and references therein.

(8) Szwarc, M. *J. Polym. Sci., Part A: Polym. Chem.* **1998**, *36*, v−xiii, and references therein.

(9) Rozenshtein, V.; Zilber, G.; Rabinovitz, M.; Levanon, H. *J. Am. Chem. Soc.* **1993**, *115*, 5193.

(10) Zilber, G.; Rozenshtein, V.; Cheng, P.-C.; Scott, L. T.; Rabinovitz, M.; Levanon, H. *J. Am. Chem. Soc.* **1995**, *117*, 10720.

(11) Fox, M. A.; Kabir-ud-Din. *J. Phys. Chem.* **1979** *83*, 1800.

(12) Hoijtink, G. J.; Zandstra, P. J. *Mol. Phys.* **1960**, *3*, 371.

(13) van Voorst, J. D. W.; Hoijtink, G. J. *J. Chem. Phys.* **1965**, *42*, 3995.

(14) van Voorst, J. D. W.; Hoijtink, G. J *J. Chem. Phys.* **1966**, *45*, 3918.

(15) Bockrath, B.; Dorfman, L. M. *J. Phys. Chem.* **1973**, *77*, 1002.

(16) Fisher, M.; Rämme, G.; Claesson, S.; Szwarc, M. *Proc. R. Soc., London A* **1972**, *327*, 481.

(17) Shenhar, R.; Willner, I.; Preda, D. V.; Scott, L. T.; Rabinovitz, M. *J. Phys. Chem. A* **2000**, *104*, 10631.

(18) Rajca, A.; Safronov, A.; Rajca, S.; Ross, C. R. II; Stezowski, J. J. *J. Am. Chem. Soc.* **1996**, *118*, 7272.

(19) Shenhar, R.; Wang. H.; Hoffman, R. E.; Frish, L.; Avram, L.; Willner. I.; Rajca, A.; Rabinovitz, M. *J. Am. Chem. Soc.* **2002**, *124*, 4685.

(20) Shenhar, R.; Beust, R.; Hagen, S.; Bronstein, H. E.; Willner, I.; Scott, L. T.; Rabinovitz, M., *J. Chem. Soc., Perkin Trans. 2* **2002**, 449.

(21) Maidan, R.; Willner, I. *J. Am. Chem. Soc.* **1986**, *108*, 1080.